2016 American Control Conference (ACC)
Boston Marriott Copley Place
July 6-8, 2016. Boston, MA, USA

Modeling the effect of nanoparticles & the bistability of transmembrane potential in non-excitable cells*

Muhammad Asif Rana[1], Ningshi Yao[1], Shayok Mukhopadhyay[2], Fumin Zhang[1], Emilie Warren[3] and Christine Payne[3]

***Abstract*— We present a simple dynamical model for the transmembrane potential in non-excitable mammalian cells. This model allows us to mimic the effect of nanoparticles on the transmembrane potential, by decreasing the permeability of potassium ion channels. We show that our model agrees with the trends observed in our experiments. However, it also exhibits opposing trends under certain conditions, which were not seen in the experiments. This indicates that the membrane potential can be bistable. We analyze the cellular conditions which may cause this apparent bistability. The effects of adding nanoparticles on sodium and chloride ion channels are also studied using the proposed model. We hypothesize that nanoparticles may also block the sodium and chloride ion channels but the extent of blockage of these ion channels may differ from that of potassium ion channels.**

I. Introduction

All mammalian cells develop a potential difference across their membranes, commonly referred to as the membrane potential or transmembrane potential. The cell membrane allows transport of ions across it through ion channels and ion pumps. However, it is selectively permeable, that is, it has ion channels that selectively allow certain ions to pass through the membrane. This selectivity develops ion concentration gradients across the membrane, which eventually cause a charge build up, and the associated potential difference [1]. At the resting membrane potential, the diffusion forces driving the ions down the concentration gradient balance out the electrical forces due to the potential difference, zeroing the net movement of ions across the membrane. While defining the membrane potential for a cell, the extracellular potential is usually considered the reference. Since the potential inside the cell is lesser compared to that outside, the resting membrane potential for a cell is usually negative. Under normal resting conditions, a cell is referred to as "polarized". A cell with resting membrane potential closer to zero is considered "depolarized", while a cell resting at a more negative membrane potential than the normal membrane potential is referred to as "hyperpolarized".

Cells are categorized as either excitable or non-excitable. A cell falls under the excitable category if it has the capability to generate an action potential. An action potential is a brief event in which the membrane potential first rapidly increases and then rapidly decreases back to its resting state [1]. Cancer cells, and other proliferating cells, are non-excitable in nature. Changes in the transmembrane potential have shown direct correlation with alteration in cell proliferation [2]. This correlation may be used to cure certain diseases, including cancer, which spread due to rapid cell proliferation. There is evidence showing an increase in growth of cancer cells with increased cell depolarization [3]. This motivates us to model the transmembrane potential in non-excitable cells such that it allows us to control the transmembrane potential. It should be noted here that most of the available literature, also discussed later in this section, is on modeling excitable cells. However, studies have shown non-excitable cells to be similar to excitable cells in terms of ionic concentrations with some difference in relative permeability of ions [9], [10], [11]. Hence, we can generalize certain aspects of these models to non-excitable cells as well.

Over the past century, many models have been proposed for the cell membrane potential. Hodgkin and Huxley [4] were the first to analyze the presence of potassium and sodium ionic currents in giant squid axons and presented an electric circuit to model the transmembrane potential and currents. The Hodgkin-Huxley model formed the basis of many more conductance-based models to follow. Connor and Stevens [5] extended this model by adding another transient potassium current to model gastropod neuron somas. Morris-Lecar[6] also presented another extended version of the Hodgkin-Huxley model for barnacle muscle fiber cells. Models for the transmembrane potential are still being proposed to better capture the dynamics of the biological system. Recently, a very useful, but complex model in [7] presented a system of differential equations to relate transmembrane potentials, ionic concentrations and cell volume of cells. Another very recent model was presented in [8] pointing out the possibility of having a bistable behavior in non-excitable cells similar to that seen in excitable cells. However, all the models mentioned above are either too complex for analysis or lack the ability to control the membrane potential through an external stimulus.

Transmembrane potential, like many other biological processes, exhibits nonlinear dynamics [12]. Examples can be

*The research work is supported by ONR grants N00014-10-10712 (YIP) and N00014-14-1-0635; and NSF grants OCE-1032285, IIS-1319874, and CMMI-1436284.

[1] Muhammad Asif Rana, Ningshi Yao and Fumin Zhang are with the School of Electrical and Computer Engineering, Georgia Institute of Technology, Atlanta, GA 30322, USA {asif.rana, zoe104yao, fumin} @gatech.edu

[2]Shayok Mukhopadhyay is with the Department of Electrical Engineering, American University of Sharjah, PO Box 26666, Sharjah, UAE smukhopadhyay@aus.edu

[3] Emilie Warren and Christine Payne are with the School of Chemistry and Biochemistry, College of Sciences, Georgia Institute of Technology, Atlanta, GA 30322, USA ewarren6@gmail.com, christine.payne@chemistry.gatech.edu

found on simulating such nonlinear biological processes [13]. Simulating the dynamics can allow better understanding of the underlying biological process [14]. Moreover, there is evidence that addition of nanoparticles in the vicinity of the cell, affects the membrane potential by blocking certain ion channels [15]. In our work, we sought to develop a nonlinear model for the transmembrane potential which is accessible to control-oriented analysis, with the control input being the addition of nanoparticles. We take inspiration from the fact that if we can control the transmembrane potential, we can control the proliferation of cancer cells and hence provide a possible cure for the disease in the future.

The aim of this paper is to come up with a simple dynamic model which allows controlling of the resting transmembrane potential of cell by regulating the permeability of its ion channels. Our model is shown to be stable over a wide range of permeability values and is seen to agree with the experimental values of resting membrane potential if certain constraints are met. The model successfully predicts the effect on membrane potential of adding nanoparticles in the vicinity of the cell. This paper provides an improvement to our earlier presented model in [16] by overcoming certain limitations mentioned later. We also show that our model exhibits a different behavior under certain set of constraints, which agrees with the work in [8]. The proposed model can also be used to study the transient behavior of transmembrane potential. Apart from that, we point out that using another set of equations mentioned in [17] leads to a model with unstable transmembrane potential.

This paper is organized in the following manner. In section II, we present the experimental results that motivate this work. Section III provides the background on existing cellular models. We present our proposed model for controlling transmembrane potential in Section IV. In Section V, we analyze the stability of the equilibrium points of the proposed model. We present the apparent bistability of the membrane potential, back our hypothesis with simulation results and compare them with experimental data in section VI. In Section VII, we further analyze our proposed model to see the possible effect of nanoparticles on the ion channels not observed in experiments. Section VIII presents the conclusion and ideas for future work.

II. Experimental Results

Experimental data was collected for two cell species: CHO (Chinese Hamster Ovary) cells and HeLa (human cervical cancer) cells. Both these cells are of the non-excitable and proliferating kind and are widely used for experimentation purposes. To set up the experiment, the cytosol of the cells were stained with green-fluorescent DiBAC$_4$(3) (bis-(1,3-dibutylbarbituric acid) trimethine oxonol). DiBAC$_4$ is known to diffuse more into the cell on increased depolarization, hence we expect an increase in the DiBAC fluorescence when the cell depolarizes. The cells were treated with different concentrations of $60nm$ amine-modified polystyrene nanoparticles and the DIBAC fluorescence was monitored using flow cytometry and fluorescence microscopy. Details

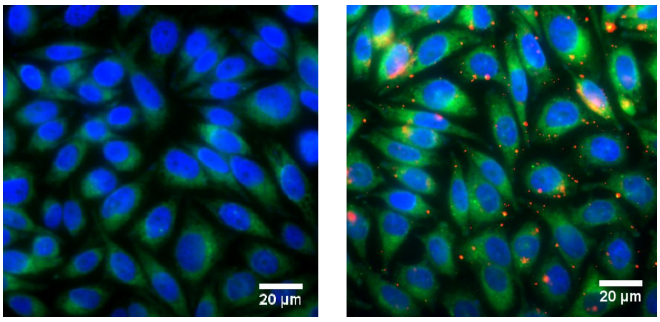

Fig. 1: Fluorescence microscopy image of CHO cells without (left) and with the introduction of red-fluorescent nanoparticles (right). Nuclei are stained with DAPI (blue) while the cytosol are stained with DiBAC$_4$(3) (green) [16].

on the experimental setup and the results are provided in [15]. Figure 1 shows the CHO cells without and with the incubation of nanaoparticles. The red-fluorescent nanoparticles bind to the exterior of the cell membrane. An increase in the green fluorescence of DIBAC is visible in the cells treated with nanoparticles. Similar trends were observed for HeLa cells.

It was concluded in the experiments that the introduction of nanoparticles causes cells to depolarize. On further investigation, it was also found that nanoparticles directly affect the permeability of potassium ion channels by blocking the channels. This causes an accumulation of positive charge inside the cell, hence causing depolarization [15].

In the sections to follow, we create a model to fit these experimental results. The next section provides the foundational models which we extend to build up our model.

III. Background

Figure 2 shows a simplified representation of a model cell under normal conditions as described in [17]. The ion channels are shown to be passages through the cell membrane that allow passive movement of three types of ions to and from the cell, that is, Cl^-(chloride), Na^+(sodium) and K^+(potassium). These channels are characterized by their relative permeability, that is, the relative ease with which the ions can flow through them. The resting membrane potential is $V_{mr} = -80mV$ for the ionic concentrations mentioned in the figure and relative permeability $P_K = 1.0$, $P_{Na} = 0.02$, $P_{Cl} = 2.0$. The figure also shows the channels being blocked by nanoparticles, depicted as red circles.

A. Hodgkin-Huxley Model

In order to model the electrical activity in cell membrane, Hodgkin and Huxley [4] presented a basic electrical circuit appropriate to model a giant squid axon as shown in Fig. 3. In this model, the membrane is represented by a capacitor with capacitance C_m, called the transmembrane capacitance. Also in the model, there is a sodium conductance G_{Na}, a potassium conductance G_K and a chloride or leakage conductance G_{Cl}. The values of these conductances depend on the relative permeability of each individual ion channel. A channel with higher permeability will have a higher value

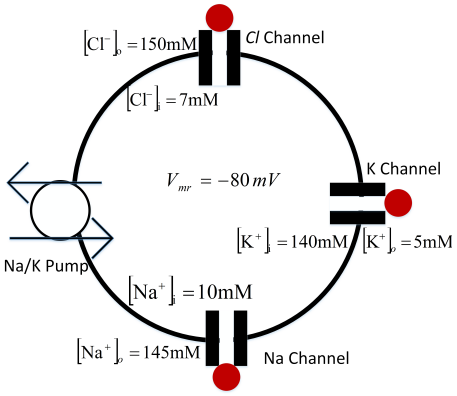

Fig. 2: A simplified representation of a cell. $[X]_i$ and $[X]_o$ refer to the intracellular and extracellular concentrations respectively of ion X. The red circles depict nanoparticles blocking the channels.

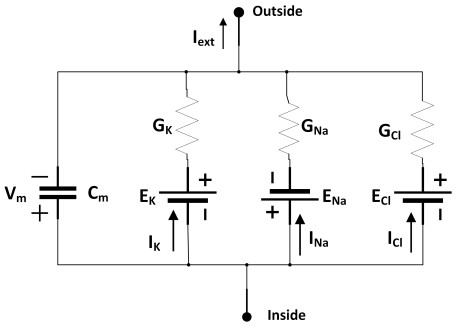

Fig. 3: The Hodgkin-Huxley membrane circuit containing Na channel, K channel and Cl channel [4]

of conductance. The membrane potential V_m is considered to be the potential inside the cell minus the potential outside the cell and all the individual channel currents I_K, I_{Na} and I_{Cl} are positive in the outward direction (leaving the cell). The individual potentials generated by each ion species are represented by batteries (E_K, E_{Na}, E_{Cl}). There is also an externally applied current in the model represented by I_{ext}. Although this model was developed for a particular type of excitable cells, the giant squid axon, it has been extended and shown to be applicable for a wide variety of cells as mentioned in Section I. Hence, we assume that this model is also applicable to the CHO and HeLa cells used in our experiments. Let's further analyze this electrical circuit.

Applying the Kirchoff's Current Law to the circuit in Figure 3 gives,

$$I_K + I_{Na} + I_{Cl} = I_{ext} - C_m\dot{V}_m \tag{1}$$

The ion channels mentioned earlier are passive channels, that is, they do not require an energy source for the transport of ions. They facilitate the movement of ions down their concentration gradients. Cells also contain active channels which make use of energy provided by sources like ATP (adnenosine triphosphate) to drive ions. One such active channel is the sodium-potassium pump. This ion pump, shown in Figure 2, exports three Na^+ ions in exchange for two K^+ ions in every cycle of operation.

Adding a term for pump current and also setting $I_{ext} = 0$ since we are not applying any external current,

$$I_K + I_{Na} + I_{Cl} + I_{pump} = -C_m\dot{V}_m \tag{2}$$

This equation needs to be satisfied by the currents and the transmembrane potential at all times.

B. Ion Channel Currents

We make use of the energy barrier model (3a) proposed in [17] to represent the various ionic currents in units of μA (microamperes). The pump current model is also taken from [17]. The currents are represented by the following set of equations,

$$\psi(t) = \frac{z_X F}{RT}V_m(t) \tag{3}$$

$$I_K(\psi(t)) = P_K F z_K([K^+]_i e^{\psi(t)} - [K^+]_o) \tag{4}$$

$$I_{Na}(\psi(t)) = P_{Na} F z_{Na}([Na^+]_i e^{\psi(t)} - [Na^+]_o) \tag{5}$$

$$I_{Cl}(\psi(t)) = P_{Cl} F z_{Cl}([Cl^-]_o e^{\psi(t)} - [Cl^-]_i) \tag{6}$$

$$I_{pump}(t) = \frac{\beta - 1}{\beta}.\frac{2.17[ATP]}{(1 + \frac{[Na^+]_c}{[Na^+]_i})^3}F \tag{7}$$

where,
$P_X(cm^3.s^{-1})$ - the relative permeability of ion channel X,
$F(Cmol^{-1})$ - the Faraday's constant,
z_X - the number of valence electrons, $z_K = z_{Na} = z_{Cl} = 1$,
$R(Jmol^{-1}K^{-1})$ - the gas constant,
$T(K)$ - the absoulute temperature,
β - the pump ratio,
$[ATP](mM)$ - the concentration of ATP (time-dependent),
$[X]_i(mM)$ - the intracellular concentration of ion X,
$[X]_o(mM)$ - the extracellular concentration of ion X,
$[X]_c(mM)$ - the half-maximal occupation concentration.

IV. The Proposed Model

We can simplify our set of equations by introducing the permeability factors, $\alpha_1 = P_K F z_K$, $\alpha_2 = P_{Na} F z_{Na}$ and $\alpha_3 = P_{Cl} F z_{Cl}$. Also let's make the substitution $k = \frac{F}{RT}$. Note that all these parameters are non-negative and bounded. Equations (4), (5), (6) can now be re-written as follows,

$$I_K(V_m(t)) = \alpha_1([K^+]_i e^{kV_m(t)} - [K^+]_o) \tag{8}$$

$$I_{Na}(V_m(t)) = \alpha_2([Na^+]_i e^{kV_m(t)} - [Na^+]_o) \tag{9}$$

$$I_{Cl}(V_m(t)) = \alpha_3([Cl^-]_o e^{kV_m(t)} - [Cl^-]_i) \tag{10}$$

Substituting the current equation (8), (9) and (10) in equation (2) gives the following,

$$\begin{aligned} -\dot{V}_m(t) = {} & \frac{e^{kV_m(t)}}{C_m}(\alpha_1[K^+]_i + \alpha_2[Na^+]_i + \alpha_3[Cl^-]_o) \\ & - \frac{1}{C_m}(\alpha_1[K^+]_o + \alpha_2[Na^+]_o + \alpha_3[Cl^-]_i) \\ & + \frac{1}{C_m}I_{pump}(t) \end{aligned} \tag{11}$$

Let's analyze the individual terms in the above equation. Since it is known that the nanoparticles effect the potassium channel permeability, we consider α_1 to be the controllable parameter. The other permeability factors α_2 and α_3 may also be effected, but since we do not have experimental evidence to justify this, we consider them fixed in our

model. In order to maintain normal operating conditions, a cell maintains the intracellular concentrations $[K^+]_i$, $[Na^+]_i$ and $[Cl^-]_i$. The extracellular concentrations $[K^+]_o$, $[Na^+]_o$ and $[Cl^-]_o$, can also be considered constant or slowly varying compared to the dynamic changes in transmembrane potential. Ion channel currents arise in order to keep these ionic concentrations constant. Moreover, in order to maintain stable chemical concentrations in the cell, the ion pump current I_{pump} has to have a relatively steady value as well. Hence, we can introduce the following constants,

$$a = \frac{1}{C_m}[K^+]_i \tag{12}$$

$$b = \frac{1}{C_m}[K^+]_o \tag{13}$$

$$c = \frac{1}{C_m}(\alpha_2[Na^+]_i + \alpha_3[Cl^-]_o) \tag{14}$$

$$d = \frac{1}{C_m}(\alpha_2[Na^+]_o + \alpha_3[Cl^-]_i - I_{pump}) \tag{15}$$

The model in (11) now becomes,

$$\dot{V}_m(t) = -(\alpha_1 a + c)e^{kV_m(t)} + \alpha_1 b + d \tag{16}$$

Considering the state variable $z(t) = e^{kV_m(t)}$, with the time derivative $\dot{z}(t) = kz(t)\dot{V}_m(t)$ and substituting equation (16),

$$\dot{z} = kz(-(\alpha_1 a + c)z + \alpha_1 b + d) \tag{17}$$

V. Stability Analysis

The system in Equation (17) has two isolated equilibrium points, $z_{01} = 0$ and,

$$z_{02} = \frac{\alpha_1 b + d}{\alpha_1 a + c} \tag{18}$$

The equilibrium point z_{01} however leads to a resting membrane potential $V_{mr} = -\infty$ which is not possible in reality. Therefore we disregard this equilibrium point. For the other equilibrium point z_{02} we can reformulate the system around this equilibrium point as,

$$\dot{z} = -kz(\alpha_1 a + c)(z - z_{02}) \tag{19}$$

To analyze the stability of the system in (19) around this equilibrium point, let's consider the Lyapunov function [18] $V = \frac{1}{2}(z - z_{02})^2$, the time derivative of which gives $\dot{V} = -kz(\alpha_1 a + c)(z - z_{02})^2$. Since $a, c > 0$ and $\alpha_1 \geq 0$ for cells under normal conditions and $z = e^{kV_m} > 0$, we notice that $\dot{V} < 0$ for all $z \in \mathbb{R}_+$ and $\dot{V} = 0$ for $z = z_{02}$. Hence, the equilibirum at $z = z_{02}$ is aymptotically stable.

Since $z_{02} = e^{kV_{mr}}$, the corresponding resting membrane potential is,

$$V_{mr} = \frac{1}{k} ln\left(\frac{\alpha_1 b + d}{\alpha_1 a + c}\right) \tag{20}$$

Equation (20) becomes equivalent to the well-known Goldman Hodgkin Katz (GHK) equation for the resting membrane potential [19] if we substitute (12), (13), (14) and (15) back in (20) and remove the pump current term I_{pump}. Although I_{pump} is not available for control, its contribution to the membrane potential becomes negligibly small when the denominator in (20) is large enough, which is the case under normal operating conditions. Hence, we can expect the resting membrane potential obtained from this model not to deviate much from the GHK equation for relatively large values of the permeability factors α_1, α_2 and α_3. For lower values of the permeability factors however, the pump current has important implications on the system. This will be shown in the section to follow.

It should also be noted here that using the ionic current model (3b) from [17] instead of (3a), results in a system with an unstable equilibrium point. This does not agree with reality since the cell membrane potential always rests at a particular value. It is also important to note that the membrane potential equation (8) in our previous work [16] disagrees with the Hodgkin-Huxley model and also the resting membrane potential provided by the associated model disagrees with the GHK equation. Our new model manages to overcome these limitations.

VI. Bistability and Simulation Results

As evident from the expression in (18), the equilibrium point z_{02} and the corresponding resting membrane potential V_{mr} are dependent on the potassium permeability factor, α_1. However, the variation in z_{02} with respect to α_1 exhibits two opposing trends under different cellular conditions. The cellular conditions here refer to the permeability factors of the ion channels other than the potassium ion channel. For the purpose of analysis, we assume that we have the capability to set these permeability factors as desired. In this section, we first provide the set of conditions which characterize the two opposing scenarios and then we go on to present them in simulation. We conclude this section by comparing the simulation results with the experimental data.

A. Bistability of the Membrane Potential

Let's consider dependence of z_{02} on α_1,

$$\frac{\partial z_{02}}{\partial \alpha_1} = \frac{bc - ad}{(\alpha_1 a + c)^2} \tag{21}$$

We see that the expression in (21) is negative if $ad > bc$, causing an increase in z_{02} and hence depolarization if α_1 is decreased. However, if $ad < bc$, a decrease in α_1 would rather cause hyperpolarization.

B. Simulation Results

The two cases mentioned in the previous subsection can be achieved by setting the permeability factors α_2 and α_3 to two different sets of desired values. This means we choose c and d in (21) to have certain constant values. However, the parameters a and b are independent of α_2 and α_3 and hence cannot be set as desired. Fixing α_2 and α_3, we vary α_1 over a range of values. A decrease in α_1 can be interpreted as adding more nanoparticles to the cell. We simulate the effect of these variations on the state variable $z(t)$ and the membrane potential $V_m(t)$.

We use the parameters, $T = 295.15K$, $R = 8.314JK^{-1}mol^{-1}$ and $F = 96485Cmol^{-1}$. The values of pump current $I_{pump} = 15pA$ and membrane capacitance $C_m = 37pF$ have been chosen in accordance with the measurements provided in [20]. The external and internal

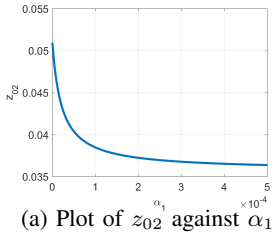

(a) Plot of z_{02} against α_1

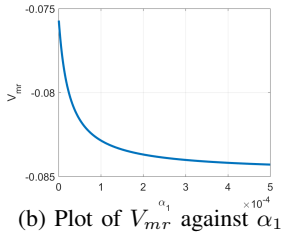

(b) Plot of V_{mr} against α_1

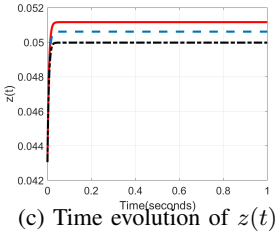

(c) Time evolution of $z(t)$

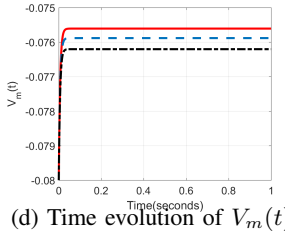

(d) Time evolution of $V_m(t)$

Fig. 4: Simulation results for case-1

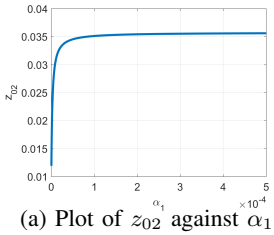

(a) Plot of z_{02} against α_1

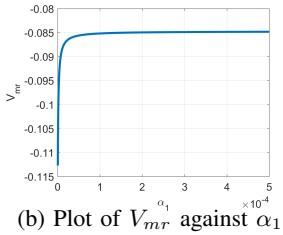

(b) Plot of V_{mr} against α_1

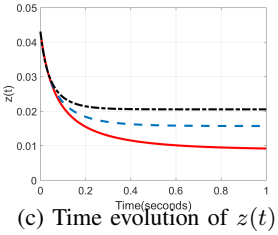

(c) Time evolution of $z(t)$

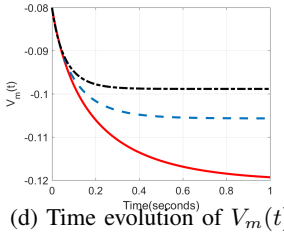

(d) Time evolution of $V_m(t)$

Fig. 5: Simulation results for case-2

ionic concentrations are taken to be the ones provided in [17], also mentioned on Figure 2.

To simulate the first scenario, we choose $\alpha_2 = 2 \times 10^{-7}$ and $\alpha_3 = 2 \times 10^{-5}$ such that $ad > bc$, and smoothly vary α_1 in the interval $[5 \times 10^{-7}, 5 \times 10^{-4}]$. Figure 4a shows how the equilibrium point z_{02} varies with increase in α_1. We notice that as α_1 becomes small, z_{02} increases, eventually approaching $\frac{d}{c} = 0.0513$. Also, since $V_{mr} = \frac{1}{k} log(z_{02})$, V_{mr} increases to $-0.076V$ as α_1 decreases as shown in Figure 4b. To simulate the transients of $z(t)$ and $V_m(t)$, we evolve the two variables with time as shown in Figures 4c and 4d respectively for a given α_1. The red-solid curve corresponds to α_1=2×10^{-7}, the blue-dashed curve represents α_1= 1×10^{-6}, while the black dash-dotted curve is for α_1=2×10^{-6}. Observing the plots reveals that z and V_m come to rest at higher values (depolarized) if α_1 is decreased.

For the other case, we make $ad < bc$ by setting $\alpha_2 = 2 \times 10^{-8}$ and $\alpha_3 = 2 \times 10^{-6}$. As in the previous case, α_1 is smoothly varied in the interval $[5 \times 10^{-7}, 5 \times 10^{-4}]$. The plots in Figure 5a and Figure 5b show the corresponding effect on z_{02} and V_{mr}. The plots for the trajectories of $V_m(t)$ and $z(t)$ for α_1=2×10^{-7} (red-solid curve), α_1= 1×10^{-6} (blue-dashed curve), α_1=2×10^{-6}(black dash-dotted curve) are also provided in Figure 5d and 5c. Unlike the previous case, it is observed that decreasing α_1 hyperpolarizes the cell rather than depolarizing it.

C. Comparison with experimental results

In Section II, we presented experimental evidence concluding that the addition of nanoparticles caused depolarization of the cells. Further experimentation identified the blocking of potassium ion channels by nanoparticles as a cause of the observed depolarization.

From the previous subsection, we see that our simulation results of the proposed model agree with the trends seen in the experiments when $ad > bc$. The parameter α_1 corresponds to the permeability of potassium ion channels and an addition of nanoparticles causes it to decrease. The simulation results for this case depict an increase in V_{mr} if α_1 is decreased, in agreement with the experimental data. On the other hand, if the cellular conditions are such that $ad < bc$, we see opposite trends as compared to the experiments.

In view of the presented simulation results, we conclude that the transmembrane potential is bistable, exhibiting either depolarization or hyperpolarization under a different set of permeability factors. The hyperpolarization state, however, is only achieved when the permeability factors become very small. The work presented in [8] also indicates the possibilty of a similar bistable behavior.

VII. Effect on Sodium and Chloride Ion Channels

Although experimental evidence suggests that nanoparticles block the potassium ion channels, we can not ignore the possible effect of adding nanoparticles on the sodium and chloride ion channels. We analyze the effect on these channels at the ionic concentrations provided in [17].

Expanding the expression for z_{02} in (18),

$$z_{02} = \frac{5\alpha_1 + 145\alpha_2 + 7\alpha_3 - 15 \times 10^{-12}}{140\alpha_1 + 10\alpha_2 + 150\alpha_3} \tag{22}$$

Computing the rate of change of z_{02} with respect and α_2 and α_3,

$$\frac{\partial z_{02}}{\partial \alpha_2} = \frac{20250\alpha_1 + 21680\alpha_3 + 15 \times 10^{-11}}{(140\alpha_1 + 10\alpha_2 + 150\alpha_3)^2} \tag{23}$$

$$\frac{\partial z_{02}}{\partial \alpha_3} = \frac{230\alpha_1 - 21680\alpha_2 + 2 \times 10^{-9}}{(140\alpha_1 + 10\alpha_2 + 150\alpha_3)^2} \tag{24}$$

Observing (24), we see that as long as the relation $21680\alpha_2 - 230\alpha_1 > 2 \times 10^{-9}$ is obeyed, we can consider the decrease in chloride ion permeability α_3 as a possible contributor to the depolarization seen in experiments. This suggests that α_2 must not be smaller than a particular limit for a given α_1. In other words, this suggests that the rate of decrease of sodium ion permeability α_2 with respect to the number of added nanoparticles, should either be decreasing with increasing nanoparticles or should remain negligibly small for any number of nanoparticles.

On the other hand, examining (23) suggests that $\frac{\partial z_{02}}{\partial \alpha_2}$ is always positive, no matter what the values of the permeability

factors are. Hence, there is no scenario where we can consider the blocking of sodium ion channels by nanoparticles as a sole contributor to the depolarization effect. However it is possible that the decrease in α_2 due to addition of nanoparticles is such that the hyperpolarization effect caused by it is always smaller as compared to the depolarization caused by a decrease in α_1 and α_3 combined under the satisfaction of the constraints mentioned earlier.

In a nutshell, analysis of the effect of individual permeability changes on z_{02} and the associated V_{mr} suggests that in order to cause cellular depolarization, nanoparticles may also block chloride ion channels apart from the potassium ion channels. They may also block the sodium ion channels but the effect is not as prominent as the other channels. Currently, we have experimental evidence for the blocking of potassium ion channels only. Further experimentation on the other ion channels will be useful to test our theoretical hypothesis.

VIII. Conclusions and Future Work

In this paper, we presented a simple dynamical system to model the transmembrane potential of biological cells. Our model allows the control of transmembrane potential by manipulating the potassium channel permeability and is shown to be stable as well. Experiments revealed that potassium channel permeability is decreased by the introduction of nanoparticles in the vicinity of the cell, causing depolarization. Hence, decrease in this permeability in simulation can be considered equivalent to adding more nanoparticles into the cell. We simulate our model for a given set of internal and external ionic concentrations and qualitatively compare the simulation trends with the experimental results. Our simulation shows the same depolarization trend for decreasing the potassium channel permeability. However, we also see opposing trends, that is, hyperpolarization of the cell under another set of conditions. This indicates a bistable behavior of the transmembrane potential. Also, theoretical analysis of the proposed model points out the possibility that nanoparticles block the sodium and chloride ion channels as well. However the extent to which the sodium and chloride ion channels are blocked may not be the same as the potassium ion channels. The model presented can be used to fit different types of cells and can enable us to predict the potassium channel permeability required to achieve a desired membrane potential. Nanoparticles can then be introduced into the cell to produce the corresponding desired permeability.

In order to find the amount of nanoparticles that should be added to achieve this desired permeability, we also need to model the dependence of ion channel permeability on the amount of nanoparticles. Moreover, we have to account for the effect of adding nanoparticles on the sodium and chloride ion channels. In the future, we propose to add more states to the system to incorporate these dynamics.

References

[1] B. Alberts, A. Johnson, J. Lewis, M. Raff, K. Roberts, and P. Walter, *Molecular Biology of the Cell*, 5th ed. Garland Science, 2007.

[2] S. Sundelacruz, M. Levin, and D. L. Kaplan, "Role of membrane potential in the regulation of cell proliferation and differentiation," *Stem cell reviews and reports*, vol. 5, no. 3, pp. 231–246, 2009.

[3] M. Yang and W. J. Brackenbury, "Membrane potential and cancer progression," *Frontiers in physiology*, vol. 4, 2013.

[4] A. L. Hodgkin and A. F. Huxley, "A quantitative description of membrane current and its application to conduction and excitation in nerve," *The Journal of physiology*, vol. 117, no. 4, pp. 500–544, 1952.

[5] J. A. Connor and C. F. Stevens, "Voltage clamp studies of a transient outward membrane current in gastropod neural somata," *The Journal of Physiology*, vol. 213, no. 1, pp. 21–30, 1971.

[6] C. Morris and H. Lecar, "Voltage oscillations in the barnacle giant muscle fiber." *Biophysical journal*, vol. 35, no. 1, p. 193, 1981.

[7] C. Poignardand, A. Silve, F. Campio, L. M. Mir, O. Saut, and L. Schwartz, "Ion fluxes, transmembrane potential, and osmotic stabilization: a new dynamic electrophysiological model for eukaryotic cells," *European Biophysics Journal*, vol. 40, no. 3, pp. 235–246, 2011.

[8] J. Cervera, A. Alcaraz, and S. Mafe, "Membrane potential bistability in nonexcitable cells as described by inward and outward voltage-gated ion channels," *The Journal of Physical Chemistry*, vol. 118, no. 43, pp. 12 444–12 450, 2014.

[9] G. Whittembury, "Sodium extrusion and potassium uptake in guinea pig kidney cortex slices," *The Journal of general physiology*, vol. 48, no. 4, pp. 699–717, 1965.

[10] J. A. Williams and D. M. Woodbury, "Determination of extracellular space and intracellular electrolytes in rat liver in vivo," *The Journal of physiology*, vol. 212, no. 1, pp. 85–99, 1971.

[11] J. A. Williams, "Effect of external K+ concentration on transmembrane potentials of rabbit thyroid cells," *American Journal of Physiology–Legacy Content*, vol. 211, no. 5, pp. 1171–1174, 1966.

[12] Y. Zhang and P. Li, "Gene-regulatory memories: Electrical-equivalent modeling, simulation and parameter identification," in *Proceedings of the 2009 International Conference on Computer-Aided Design*. ACM, 2009, pp. 491–496.

[13] M. Jackson and J. Gnadt, "Numerical simulation of nonlinear feedback model of saccade generation circuit implemented in the labview graphical programming language," *Journal of neuroscience methods*, vol. 87, no. 2, pp. 137–145, 1999.

[14] Y. Zhang, P. Li, and G. M. Huang, "Quantifying dynamic stability of genetic memory circuits," *Computational Biology and Bioinformatics, IEEE/ACM Transactions on*, vol. 9, no. 3, pp. 871–884, 2012.

[15] E. A. K. Warren and C. K. Payne, "Cellular binding of nanoparticles disrupts the membrane potential," *RSC Advances*, vol. 5, pp. 13 660–13 666, 2015.

[16] S. Mukhopadhyay, F. Zhang, E. Warren, and C. Payne, "A model for controlling the resting membrane potential of cells using nanoparticles," in *53rd IEEE Annual Conference on Decision and Control (CDC)*, Dec 2014, pp. 6017–6022.

[17] C. M. Armstrong, "The Na/K pump, Cl ion, and osmotic stabilization of cells," *Proceedings of the National Academy of Sciences*, vol. 100, no. 10, pp. 6257–6262, 2003.

[18] H. K. Khalil, *Nonlinear Systems*, 3rd ed. Prentice Hall, 2002.

[19] A. L. Hodgkin and B. Katz, "The effect of sodium ions on the electrical activity of the giant axon of the squid," *The Journal of physiology*, vol. 108, no. 1, pp. 37–77, 1949.

[20] R. Dipolo and A. Marty, "Measurement of na-k pump current in acinar cells of rat lacrimal glands." *Biophysical Journal*, vol. 55, no. 3, p. 571, 1989.